e-ISSN 2320 –7876 www.ijfans.org
Vol.11, Iss.9, Dec 2022

Synthesis and Characterization of Mn_2O_3 nanoparticles for photocatalytic application

R. Rekha[1], G. Gurumoorthy[1*],
[1]Department of Chemistry, Faculty of Arts & Science,
Bharath Institute of Higher Education & Research, Selaiyur, Chennai-73, Tamilnadu, India
Email-gurumoorthychemistry.cbcs@bharathuniv.ac,in

Address for Correspondence

R. Rekha[1], G. Gurumoorthy[1*],
[1]Department of Chemistry, Faculty of Arts & Science,
Bharath Institute of Higher Education & Research, Selaiyur, Chennai-73, Tamilnadu, India
Email-gurumoorthychemistry.cbcs@bharathuniv.ac,in

Abstract

The synthesis of Manganese(III) oxide nanoparticles (Mn_2O_3NPs) was by visible light assisted approach using the TMA.OH, $H_2O_2$and metal precursor aqueous solution of $MnCl_2\cdot4H_2O$. The formation of dark brown suspension was placed one day in the atmospheric air for the formation of the product via precipitation method during a process the product was accompanied by O_2 gas generation. Dried aggregate was separated by filtration, washed with higherquantity of deionized water and methyl alcohol, and then dried at 80˚C for 16 h in air and finely were heated at 500 ˚C for 5 h. After the preparation Mn_2O_3NPs was tested using the following instrumental techniques such as UV-vis., FT-IR, XRD, FE-SEM. In this present investigation, Mn_2O_3NPs uses as photocatalyst over the degradation of Rhodamine B.

Key words: Mn_2O_3NPs, Visible light assisted method, Photocatalytic degradation, Rhodamine B

1.Introduction

Transition metal oxides are a broad class of materials possesses important features and explored in different fields [1-9]. Here, Manganese oxide is a n-type non-stoichiometric semiconductor which exists in different polymorphic and crystallographic forms and it exist in different oxidation state like MnO, MnO_2, Mn_2O_3, Mn_3O_4, and Mn_5O_8 with 1D, 2D, and 3D morphologies like rod, wire, cubes, spheres, urchins, sheets , flowers and many more. Based on earlier report some of the preparation methods could be adopted for the synthesis of manganese oxide like sol-

e-ISSN 2320 –7876 www.ijfans.org
Vol.11, Iss.9, Dec 2022

gel method, electrospinning, solid state, ion-exchange, precipitation and co-precipitation techniques, thermal decomposition and many more [10-25].

Among them, co-precipitation technique is the most common method for the synthesis of nano/microstructure because different parameters are play a vital role in this method like reaction temperature, initial concentration of materials, pH of the solution and its reaction temperature to get desired size and shapes [26-38]. Here, etramethylammonium hydroxide (TMAOH) used as surfactant as well as surface modifying agent used to growth of the nanostructures and the effect of adding TMAOH with metal precursor it leads to the formation of well dispersed manganese oxide. In this present investigation, the prepared manganese oxide is uses as a photocatalyst for the removal of organic pollutant like Rhodamine B (RhB) by photodegradation. Now a days, the rapid increases of the human population and higher number industries are directly affect our environment, resulting in the depletion of natural resources by sending the effluent without any purification in the freshwater resources. Some common techniques like physical, chemical and biological methods are available for the removal of organic dyes but the physical and biological methods not remove completely it only can transfer its phase and some chemical methods like ozonation and chlorination has some limitation to environment [39-43]. So the photocatalysis is the efficient one to destroyed the dye when bombarded by UV irradiation. Rhodamine B is xanthenes organic dye which dissolves easily in water and also it’s a highly allergic to the eyes, skin and our respiratory system because it is well recognized water tracer fluorescent materials. As a result, preventing dye wastewater pollution is a critical issue that must be addressed globally.

2. Experimental Section

2.1. Reagents

$MnCl_2$, Tetramethylammoniumhydroxide (TMA.OH) were purchased from Aldrich chemicals. Othe the all-remaining chemicals were obtained from locally available in analytical grade used as received and only the Millipore water was used to prepare all the stock solutions for all measurements.

e-ISSN 2320 –7876 www.ijfans.org
Vol.11, Iss.9, Dec 2022

2.2. Preparation of MnO_2 and Mn_2O_3Nanoparticles

The preparation of MnO_2 nanoparticles was by the addition of 40 mL of a aqueous solution(1.2 M Tetramethylammonium hydroxide **(**TMA.OH)) is mixed with 6 wt % H_2O_2 was added to 20 mL of aqueous 0.6 M $MnCl_2{\cdot}4H_2O$ solution within 30 s. The formed dark browncoloured suspension was placed in a visible light one day in the open atmospheric air, which is accompanying of O_2 gas generation.The copious amount of Millipore water used to separate the dried aggregate by filtration, washed with thoroughly with higher quantity of deionized H_2O, CH_3OH, and air-dried at 80 °C for 6 h and then the MnO_2 was converted in to Mn_2O_3 via thermal decomposition at 450-500 °C, finely obtained the nanopowder of Mn_2O_3 for the further analysis.

2.3.Instrumentation

The electronic spectra of synthesised Mn_2O_3NPs were obtained using a SHIMADZU-1800 (UV-Vis. Spectrophotometer) from Japan and the FT-IR spectra from a Perkin Elmer Y-40 from the United States. Philips, JSO debye Flex 2002 Seifert with 10°/min scanning speed was used to evaluate the XRD pattern. HITACHI, SU6600 with voltage (0 kV (FE-SEM), Japan, validated the morphology, size, and forms of the nanoparticles. HR-TEM pictures were taken with a JEOL-3010 device.

3. Results and Discussions

Figure 1 shows UV-Visible spectra of Mn_2O_3NPs synthesized by co-precipitation method followed by the thermal decomposition. The analysis a few mg of Mn_2O_3NPs was dispersed in Millipore water using ultrasonic probe. There is no visible absorption obtained but one band was obtained at 393 nm due to the effect of quantumconfinement and this confirmed the synthesize of Mn_2O_3NPs nanoparticles by using this route successfully in very smaller size of the particles due to its large surface area it has very good optical activity [29, 32].

e-ISSN 2320 –7876 www.ijfans.org
Vol.11, Iss.9, Dec 2022

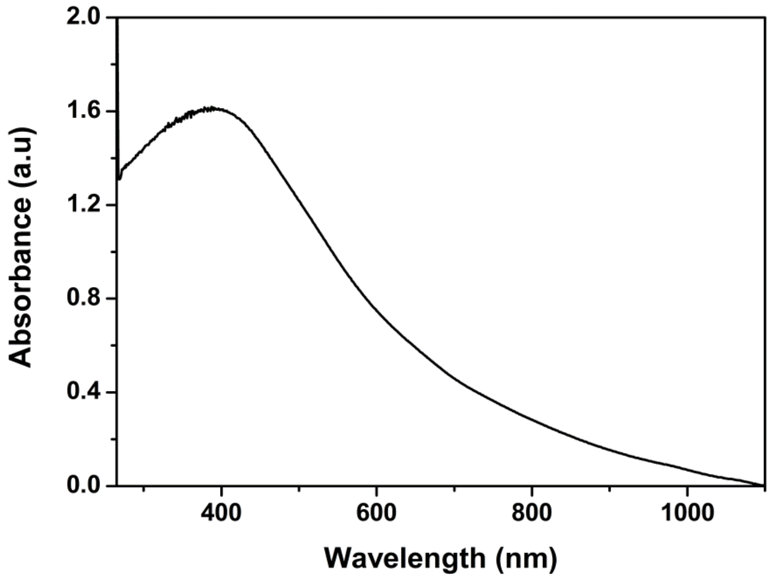

Fig. 1:UV-Visible spectrum of Mn_2O_3NPs.

Fig. 2 represents the FT-IR spectrum of the Mn_2O_3NPsnanoparticles prepared by co-precipitation method followed by the thermal decomposition. furthermore, the bands obtained at 1640, 3417 cm^{-1} correspond to the presence of higher numbers of residual hydroxyl groups, which entail the O-H vibrationalbending mode and stretching vibrations of adsorbed water in trace level. The band presented at 463, 509 cm^{-1} can attributed to the Mn-O vibrations of Mn_2O_3NPs nanoparticles [25, 27].

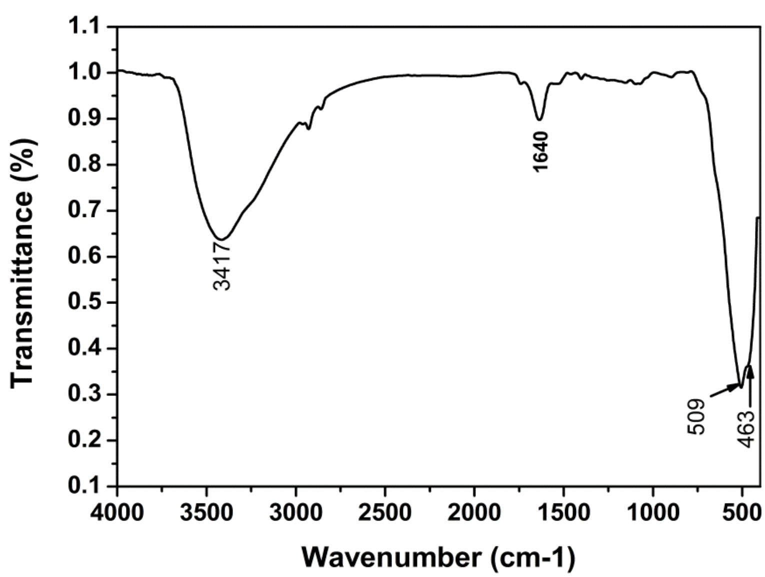

e-ISSN 2320 –7876 www.ijfans.org
Vol.11, Iss.9, Dec 2022

Fig. 2:FT-IR spectrum of Mn_2O_3NPs.

Figure 3 shows XRD pattern of the Mn_2O_3NPsnanoparticles prepared using co-precipitation method followed by the thermal decomposition approach. The typical XRD patterns show broad diffraction peaks observed at 23.0, 32.5, 38.1, 44.5, 51.0, 56.1, 59.6 and 64.9 which are corresponding to Braggs reflections from (121), (104), (004), (332), (341), (404), (161) and (226) planes which corresponds to Mn_2O_3NPsnanoparticle [25]s. From the XRD pattern it is clear that Mn_2O_3NPsnanoparticlessynthesized were purely crystalline in nature. Uniform particle sizes of Mn2O3NPs were obtained between to be 20-25 nm was calculated using Scherrer equation.

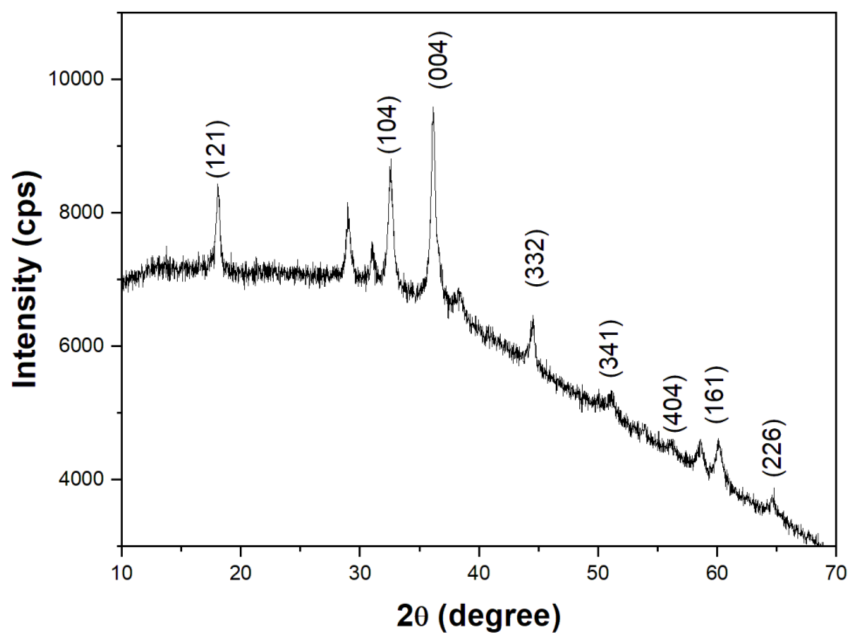

Fig.3:XRD spectrum of Mn_2O_3NPs

The morphology of Mn_2O_3NPs nanoparticles was examined with different resolution by FE-SEM. Some amount of Mn_2O_3NPs nanoparticles dispersed in water using ultrasonic probe and coated on carbon tape for the analysis [31]. Fig. 4 shows the Mn_2O_3NPs nanoparticles consist almostcoarse like arrangements in micro arrangements and clearly noted in HR-TEM images it almost spheres like structure of Mn_2O_3NPsand its EDS confirms the prepared samples have only manganese and oxide are predominantly present in Mn_2O_3NPsis clearly view from the percentile table.

e-ISSN 2320 –7876 www.ijfans.org
Vol.11, Iss.9, Dec 2022

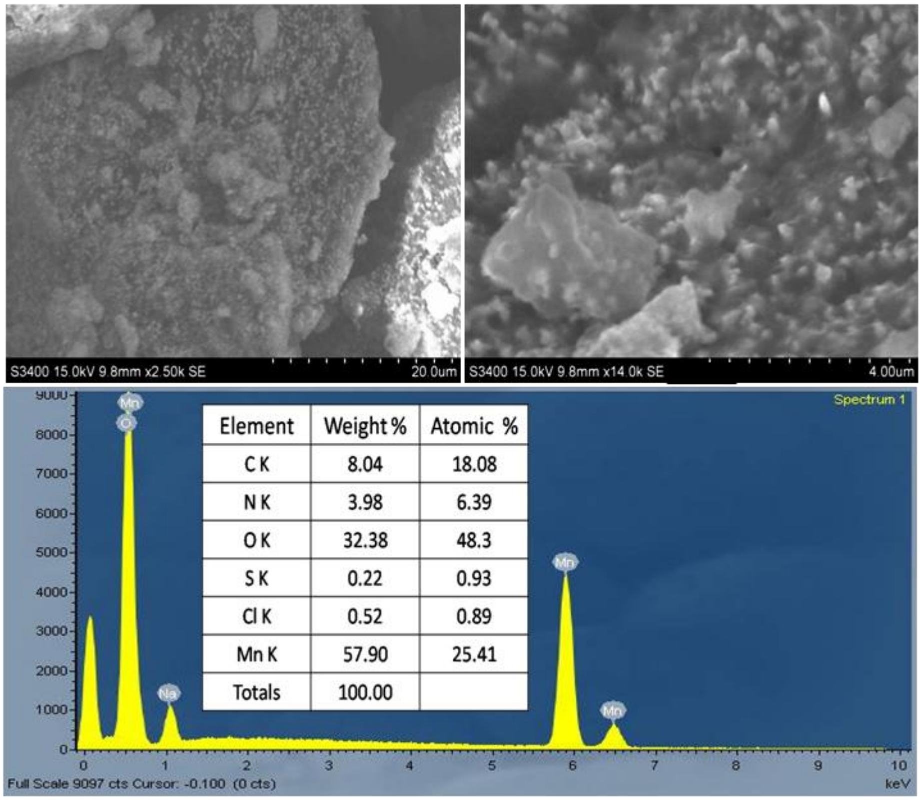

Fig. 4:FE-SEM images of Mn_2O_3NPsalong with EDAX and its percentile table.

The photocatalytic activity of the Mn_2O_3NPs was evaluated using photo degradation of an aqueous RhB textile dye is shown in Fig.5a. The experiment carried out in a cylindrical double-walled hollow photo reactor with water circulation facility. A 20 W UV lamp (wavelength of 352 nm) was place inside the reactor. The catalytic experiments carried out with 100 mL solution of 1.0 X 10^{-5} M concentration of RhB dye and 100 mg of the Mn_2O_3NPs catalyst under constant stirring. About 3 mL of the aliquot solution withdrawn at predetermined time intervals (15 mins) from the reaction mixture, centrifuged and the decrease in absorbance values monitored [37-43]. The pseudo first order rate constants (1) were calculated from the slopes of the plots of ln C_0/C vs time. The percentage reduction of dye were calculated using the following expressions (2).

$$k = \frac{2.303}{t} \ln \frac{C_0}{C} \qquad \text{... (1)}$$

$$\text{Percentage reduction} = \frac{\text{O.D. at initial time } (C_0) - \text{O.D. at time } t(C_t)}{\text{O.D. at initial time } (C_0)} \times 100 \qquad \text{... (2)}$$

where, C_o = initial concentration of the dye solution, C_t = concentration remaining after irradiation at time t.

and the relationship between $\ln(C_0/C_t)$ and degradation time shows a linear relationship which suggest that the degradation of RhB is a first-order reaction in Fig.5b. The apparent rate constants obtained as 3.2 $x10^{-3}$ min-1 for absence of catalyst and presence of Mn_2O_3NPs from the slope of ln (C0/Ct) versus degradation time.

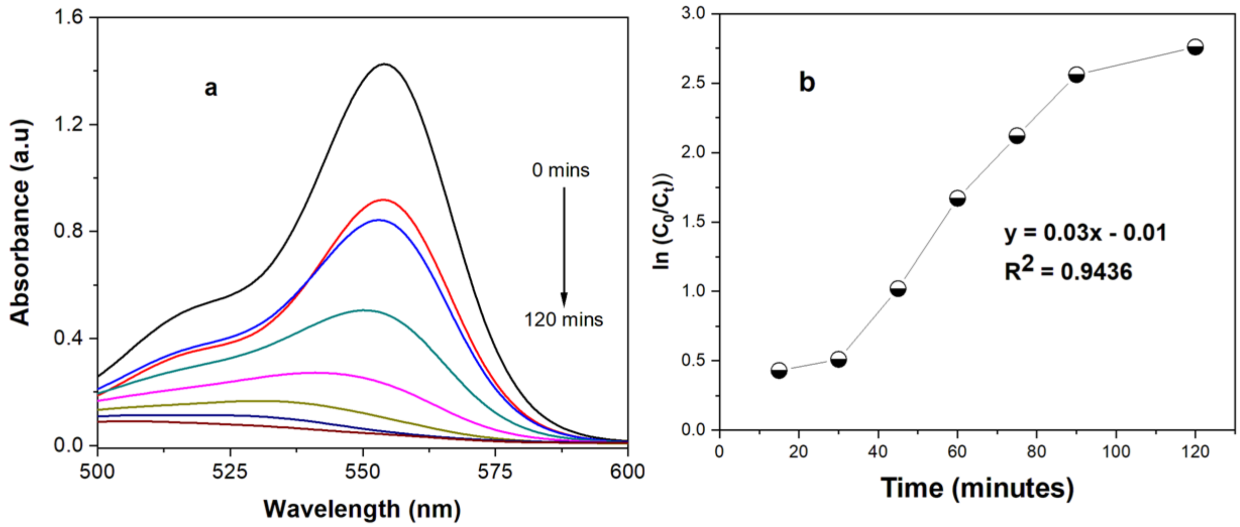

Fig. 5: UV-visible spectra for the photocatalytic degradation of RhB (a) and its calibration plot (b).

The reduction efficiency in reuseability of Mn_2O_3NPs (Fig.6) has confirmed by doing for 5 cycles the degradation of RhB without change of the catalyst. This process continued five times without any evident loss of its catalytic activity. The catalytic efficiency of the heterogeneous catalyst is found to be maintained without any loss in each cycle due to the inherent stabilization of Mn_2O_3NPs.

e-ISSN 2320 –7876 www.ijfans.org
Vol.11, Iss.9, Dec 2022

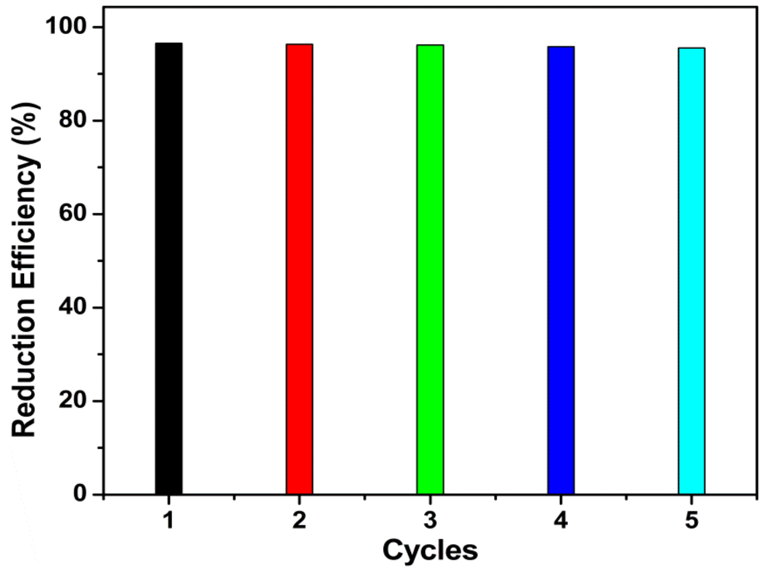

Figure 9: Reusability of ZnO nanospheres.

4. conclusion

The synthesis of Manganese(III) oxide nanoparticles (Mn_2O_3NPs) was by visible light assisted method using TMA.OH, H_2O_2 and metal precursor aqueous solution of $MnCl_2 \cdot 4H_2O$. The formation of dark brown precipitate was placed one day in the atmospheric air for the formation of the product via precipitation method during a process the product was accompanied by O_2 gas generation. Dried aggregate separated by filtration, washed with higherquantity of distilled water and CH3OH, and then dried at 80˚C for 16 h in air.The prepared MnO_2 for the conversion of Mn_2O_3NPs were heated at 500 ˚C for 5 h.The prepared Mn_2O_3NPs analyzed using various instrumental techniques such as UV-vis., FT-IR, and also the morphology, shape, size, composition of the metal oxide, which was determined by the following techniques such as XRD, FE-SEM studies.

The prepared Mn_2O_3NPs were analyzed using different analytical techniques and which are confirmed Mn_2O_3NPs formed like course structures which have nearly 20-25 nm in size with high purity with high surface area to subject as catalyst for the degradation of organic pollutant. Mn_2O_3NPs used as a heterogeneous catalyst for the photodegradation of Rhodamine B and performed very well with degrading ability nearly 96% at 120 mins of exposure. The apparent rate constants obtained as 3.4 $x10^{-3}$ min-1 for absence of catalyst and presence of Mn_2O_3NPs

e-ISSN 2320 –7876 www.ijfans.org
Vol.11, Iss.9, Dec 2022

nanocatalysts, respectively.Based on the above considerations, we developed a cost effective photocatalyst for degradation of different organic dye contaminants.

References:

1. C. Julien, A. Mauger, Nanostructured MnO2 as Electrode Materials for Energy Storage, Nanomaterials. 7 (2017) 396.
2. R. Ponnusamy, R. Venkatesan, M. Kandasamy, B. Chakraborty, C. Rout, MnO2 polymorph selection for non-enzymatic glucose detection: An integrated experimental and density functional theory investigation, Applied Surface Science. 487 (2019) 1033-1042.
3. W. Guo, C. Yu, S. Li, Z. Wang, J. Yu, H. Huang, J. Qiu, Strategies and insights towards the intrinsic capacitive properties of MnO2 for supercapacitors: Challenges and perspectives, Nano Energy. 57 (2019) 459-472.
4. Rafique, A. Massa, M. Fontana, S. Bianco, A. Chiodoni, C.F. Pirri, S. Herna´ndez, A. Lamberti, Highly uniform anodically deposited film of MnO2 nanoflakes on carbon fibers for flexible and wearable fiber-shaped supercapacitors. ACS Appl. Mater. Interfaces 9 (2017) 28386 –28393.
5. X. Shi, Y. Li, R. Chen, H. Ni, W. Zhan, B. Zhang, F. Zheng, S. Dong, Defective carbon nanotube forest grown on stainless steel encapsulated in MnO2 nanosheets for supercapacitors. Electrochim. Acta 278 (2018) 61-71.
6. J. Wang, F. Kang, B. Wei, Engineering of MnO2-based nanocomposites for high-performance supercapacitors, Progress In Materials Science. 74 (2015) 51-124.
7. X. Li, R. Ding, W. Shi, Q. Xu, L. Wang, H. Jiang, Z. Yang, E. Liu, Hierarchical mesoporous Ni-P@MnO2 composite for high performance supercapacitors. Mater. Lett. 187(2017) 144-147.
8. Q.J. Le, T. Wang, D.N.H. Tran, F. Dong, Y.X. Zhang, D. Losic, Morphology-controlled MnO2 modified silicon diatoms for high-performance asymmetric supercapacitors, J. Mater. Chem. A, 5 (2017) 10856-10865.
9. J. Cao, X. Li, Y. Wang, F.C. Walsh, J.H. Ouyang, D. Jia, Y. Zhou, Materials and fabrication of electrode scaffolds for deposition of MnO2 and their true performance in supercapacitors, Journal Of Power Sources. 293 (2015) 657-674.

e-ISSN 2320 –7876 www.ijfans.org
Vol.11, Iss.9, Dec 2022

10. R. Sundari, S. Alva, D. Sebayang, H. Wahyudi, S. Jonit, A. Kamaruddin, Characterization of fabricated MnO2-amberlite photocatalyst by FTIR, XRD and SEM for alizarin removal. IOP Conf. Ser.: Mater. Sci. Eng. 343(2018) 012003
11. J. Zhao, J. Nan, Z. Zhao, N. Li, J. Liu, F. Cui, Energy-efficient fabrication of a novel multivalence Mn3O4-MnO2 heterojunction for dye degradation under visible light irradiation, Applied Catalysis B: Environmental. 202 (2017) 509-517.
12. W. Si, Y. Wang, Y. Peng, X. Li, K. Li, J. Li, A high-efficiency c-MnO2-like catalyst in toluene combustion. Chem. Commun. 51 (2015) 14977-14980.
13. A. Shalini, P. Paulraj, K. Pandian, G. Anbazhagan, V. Jaisankar, Synthesis and Characterization of Graphene Oxide Coated Au Nano Particles and The Study of its Application on Electro Catalytic Activity of Nitric Oxide, Advanced Materials Proceedings, 4(4) (2019) 158-161.
14. L. Han, C. Shao, B. Liang, A. Liu, Genetically engineered phage-templated MnO_2 nanowires: synthesis and their application in electrochemical glucose biosensor operated at neutral pH condition. ACS Appl. Mater. Interfaces 8 (2016) 13768–13776.
15. L. Zhang, Q. Chen, X. Han, Q. Zhang. MnO_2 Nanoparticles and Carbon Nanofibers Nanocomposites with High Sensing Performance Toward Glucose. Journal of Cluster Science 29 (2018) 1089-1098.
16. S. Zhang, J. Zheng, Synthesis of single-crystal a-MnO2 nanotubes-loaded Ag@C core–shell matrix and their application for electrochemical sensing of nonenzymatic hydrogen peroxide. Talanta 159 (2016) 231-237.
17. N. Kumar, S. Bhaumik, A. Sen, A.P. Shukla, S.D. Pathak, One-pot synthesis and first-principles elasticity analysis of polymorphic MnO2 nanorods for tribological assessment as friction modifiers. RSC Adv. 7 (2017) 34138-34148.
18. T. Zhang, L. Kong, Y. Dai, X. Yue, J. Rong, F. Qiu, J. Pan, Enhanced oils and organic solvents absorption by polyurethane foams composites modified with MnO2 nanowires. Chem. Eng. J. 309 (2017) 7-14.
19. S. Blessi, Ayyar Manikandan, S. Anand, M.M.L. Sonia, V. Maria Vinosel, P. Paulraj, Y. Slimani, M.A. Almessiere, M. Iqbal, S. Guner, A. Baykal, Effect of zinc substitution on the physical and electrochemical properties of mesoporous SnO2 nanoparticles, Materials Chemistry and Physics 273 (2021) 125122.

e-ISSN 2320 –7876 www.ijfans.org
Vol.11, Iss.9, Dec 2022

20. Y. Wang, P. Ding, C. Wang, Fabrication and lithium storage properties of MnO2 hierarchical hollow cubes. J. Alloys Compd. 654 (2016) 273-279.
21. Y. Zhang, F. Wang, P. Ou, H. Zhu, Y. Lai, Y. Zhao, W. Shi, Z. Chen, S. Li, T. Wang, High efficiency and rapid degradation of bisphenol A by the synergy between adsorption and oxidization on the MnO2@nano hollow carbon sphere. J. Hazard. Mater. 360 (2018) 223-232.
22. S.Y. Qi, J. Feng, J. Yan, X.Y. Hou, M.L. Zhang, Hydrothermal synthesis and supercapacitor properties of urchin sphere and nanowire MnO2. Chin. J. Nonferrous Met. 18 (2008) 113-117.
23. Y. Zhang, Z. Yang, M. Li, L. Yang, J. Liu, Y. Ha, R. Wu, Heterostructured CoFe@C@MnO2 nanocubes for efficient microwave absorption. Chem. Eng. J. 382 (2020) 123039.
24. Y. He, D. Bin Jiang, J. Chen, D.Y. Jiang, Y.X. Zhang, Synthesis of MnO2 nanosheets on montmorillonite for oxidative degradation and adsorption of methylene blue. J. Colloid Interface Sci. 510 (2018) 207-220.
25. P. Paulraj, Ahmad Umar, K. Rajendran, A. Manikandan, A. Sathamraja, R. Kumar, E. Manikandan, K. Pandian, S. Baskoutas, Hassan Algadi, Ahmed A. Ibrahim, Mabkhoot A. Alsaiari, Methylene blue intercalated layered MnO_2 nanosheets for high-sensitive non-enzymatic ascorbic acid sensor, J. Mater Sci: Mater Electron, 3 (2021) 1-13.
26. Moharreri, E.; Hines, W. A.; Biswas, S.; Perry, D. M.; He, J.;Murray-Simmons, D.; Suib, S. L. Comprehensive Magnetic Study of Nanostructured Mesoporous Manganese Oxide Materials and Implications for Catalytic Behavior. Chem. Mater. 30 (2018) 1164−1177.
27. Zhao, J.; Nan, J.; Zhao, Z.; Li, N. Facile Fabrication of Novel Mn2O3 Nanocubes with Superior Light-Harvesting for Ciprofloxacin Degradation. Catal. Commun. 102 (2017) 5−8.
28. Jassby, D.; Farner Budarz, J.; Wiesner, M. Impact of Aggregate Size and Structure on the Photocatalytic Properties of TiO2 and ZnO Nanoparticles. Environ. Sci. Technol. 46 (2012) 6934−6941.
29. K.S.Pugazhvadivu, K.Ramachandran, K.Tamilarasan, Synthesis and Characterization of Cobalt doped Manganese Oxide Nanoparticles by Chemical Route, Physics Procedia 49 (2013) 205 – 216.

e-ISSN 2320 –7876 www.ijfans.org
Vol.11, Iss.9, Dec 2022

30. Shulin Chen, Fan Liu, Quanjun Xiang, Xionghan Feng, Guohong Qiu, Synthesis of Mn2O3 microstructures and their energy storage ability studies, Electrochimica Acta, 106 (2013) 360-371.
31. X. Niu, H. Wei, K. Tang, W. Liu, G. Zhao, Y. Yang, Solvothermal synthesis of 1D nanostructured Mn2O3: effect of Ni2+ and Co2+ substitution on the catalytic activity of nanowires, this: RSC Adv. 5 (2015) 66271-66277.
32. Esraa Kareem Jassem, Aseel Mustafa Abdul Majeed, Nibras Mossa Umran, The Effect of Temperature on Structural and optical properties of Manganese Oxide Nanoparticles, Journal of Physics: Conf. Series 1279 (2019) 012004
33. R. Najjar, R. Awad, A. M. Abdel-Gaber, Physical Properties of Mn2O3 Nanoparticles Synthesized by Co-precipitation Method at Different pH Values, J Supercond Nov Magn., 32 (2019) 885–892.
34. A.D. Khalaji, M. Ghorbani, Mn2O3 Nanoparticles Synthesized from Thermal Decomposition of Manganese(II) Schiff Base Complexes, Acta Physica Polonica Series a 133 (2018) 7-9.
35. Z. S. Sadeq, Structural and Optical Study of Mn2O3 Nanoparticles and its Antibacterial Activity, 161 (2019) 76-84.
36. P. Paulraj, Ahmad Umar, K. Rajendran, A. Manikandan, R. Kumar, E. Manikandan, K. Pandian, Mater H.Mahnashi, Mabkhoot A.Alsaiari, Ahmed A.Ibrahim, Nikolaos Bouropoulos, Sotirios Baskoutas, Solid-state synthesis of Ag-doped PANI nanocomposites for their end-use as an electrochemical sensor for hydrogen peroxide and dopamine, Electrochimica Acta, 363(2020) 137158.
37. B. Abebe, E. A. Zereffa, H C A. Murthy, Synthesis of Poly(vinyl alcohol)-Aided ZnO/MnO Nanocomposites for Acid Orange-8 Dye Degradation:Mechanism and Antibacterial Activity, ACS Omega, 6 (2021) 954-964.
38. C. Kalaiselvi, M. Ramesh Aravind, B.Revathi, A. Nirmala Grace, P. Sudhagar, N. R. Krishna Chandar, Long single crystalline α-Mn2O3 nanorods: facile synthesis and photocatalytic application, Mater. Res. Express 7 (2020) 074001.
39. R. Marx Nirmal, P. Paulraj, K. Pandian, K. Sivakumar, Preparation, Characterization and Photocatalytic Properties of CdS and Cd1-xZnxS nanostructures, AIP Conf. Proc. 1391 (2011) 597-599.

e-ISSN 2320 –7876 www.ijfans.org
Vol.11, Iss.9, Dec 2022

40. R. Saravanan, H. Shankar, G. Rajasudha, A. Stephen, photocatalytic degradation of organic dye using nano ZnO, International Journal of Nanoscience, 10 (2011) 253-257.
41. P. AnnieVinosha, A. Manikandan, R. Ragu, A. Dinesh, P. Paulraj, Y. Slimani, M. A. Almessiere, A. Baykal, J. Madhavan, B. Xavier, G. F. Nirmala, Exploring the influence of varying pH on structural, electro-optical, magnetic and photo-Fenton properties of mesoporous $ZnFe_2O_4$ nanocrystals, Environmental Pollution, 2020, 115983.
42. G. Gurumoorthy, S. Thirumaran, Rajram Arulmozhi and S. Ciattini, Synthesis of nickel sulfide and nickel-iron sulfide nanoparticles from nickel dithiocarbamate complexes and their photocatalytic activities, Appl Organometal Chem. 2020;**34**:e5761
43. G. Gurumoorthy, G. Mathu Bala, R. Hema. (2021). Synthesis Andcharacterization of Zinc Sulfide and Zinc-Iron Sulfide Nanoparticles from Zinc (II) Dithiocarbamate Complexes. Annals of the Romanian Society for Cell Biology, *25*(2), 2091–2095.